PHYSICAL REVIEW B VOLUME 59, NUMBER 16 15 APRIL 1999-II

Interdiffusion in nanometer-scale multilayers investigated by *in situ* low-angle x-ray diffraction

Wei-Hua Wang*
Institute of Physics, Chinese Academy of Sciences, Beijing 100080, China

Hai Yang Bai
Cryogenic Laboratory, Chinese Academy of Sciences, Beijing 100080, China

Ming Zhang, J. H. Zhao, X. Y. Zhang, and W. K. Wang
Institute of Physics, Chinese Academy of Sciences, Beijing 100080, China

(Received 22 July 1998; revised manuscript received 9 November 1998)

An *in situ* low-angle x-ray diffraction technique is used to investigate interdiffusion phenomena in various metal-metal and metal-amorphous Si nanometer-scale compositionally modulated multilayers (ML's). The temperature-dependent interdiffusivities are obtained by accurately monitoring the decay of the first-order modulation peak as a function of annealing time. Activation enthalpies and preexponential factors for the interdiffusion in the Fe-Ti, Ag-Bi, Fe-Mo, Mo-Si, Ni-Si, Nb-Si, and Ag-Si ML's are determined. Activation enthalpies and preexponential factors for the interdiffusion in the ML's are very small compared with that in amorphous alloys and crystalline solids. The relation between the atomic-size difference and interdiffusion in the ML's are investigated. The observed interdiffusion characteristics are compared with that in amorphous alloys and crystalline α-Zr, α-Ti, and Si. The experimental results suggest that a collective atomic-jumping mechanism govern the interdiffusion in the ML's, the collective proposal involving 8–15 atoms moving between extended nonequilibrium defects by thermal activation. The role of the interdiffusion in the solid-state reaction in the ML's is also discussed. [S0163-1829(99)01516-7]

I. INTRODUCTION

Multilayers (ML's) are of technologically useful physical properties and potential application in microelectronic device.[1–3] ML's can also provide a model system for scientists to investigate fundamental phenomena such as interface properties, stabilization of nonequilibrium structure and strains, and coupling interactions in magnetism and transport behavior. Therefore, the interdiffusion study in the compositionally modulated ML's are interesting subjects.[3–7] From a scientific point of view the diffusion mechanism in ML's is still poorly understood, and a knowledge of the interdiffusion data and mechanism is highly desired for understanding the physical properties and phenomena in the ML's. From a technological viewpoint, the knowledge of the interdiffusion is an important prerequisite for application of the ML's. The discovery of solid-state interfacial reaction (SSIR) in the thin films has further added to the importance of interdiffusion investigations in these materials. However, despite many years of effort, the interdiffusivity in the ML's has remained poorly quantified.[7] This is because of the measurement difficulties associated with low diffusivity (less than $10^{-23}\,m^2/s$) in the ML's at low-annealing temperature. The difficulties are even higher in the amorphous ML's because the measurements must be done at a sufficiently low temperature to avoid crystallization in amorphous ML's. The difficulties inherent to diffusion experiments in amorphous ML's can also be due to the metastability, which implies small mean-squared displacements. Rutherford backscattering (RBS), Auger electron spectroscopy (AES), and secondary-ion-mass spectrometry, which are normally used to measure the diffusivity in thin film are difficult to measure diffusion coefficient less than $10^{-23}\,m^2/s$, which is often the case for the ML's.[8] The measuremental data often scatter so much that they cannot be used to deduce reliable information on the temperature dependence of interdiffusivities. A low-angle x-ray diffraction (XRD) technique based on the linearized diffusion theory has been used to study the interdiffusion phenomena in multilayer systems.[9,10] The interdiffusion information is obtained by carefully monitoring the intensity changes of the low-angle XRD modulation peak as a function of annealing time. This is the most sensitive technique available for measuring diffusivities as low as $10^{-27}\,m^2/s$ in ML's with a modulation period of a few nanometers. Results from this technique have been reviewed extensively.[7] The method, originally developed for crystalline materials, has been successfully applied to measure diffusivities in amorphous ML's.[11,12] Despite the fact that a considerable amount of interdiffusion measurements have been carried out in the ML's, however, there are too limited systematic investigations to permit conclusion on the diffusion mechanism in the ML's.[9–18] On the other hand, a series of ML's, mostly metal-metal (M-M) ML's and metal-Si (M-Si) ML's, has been discovered in which the amorphization reaction is attainable by interdiffusion. Reviews on the SSIR in the ML's are given by Johnson[19] and Samwer.[20] The SSIR would also decrease the composition gradient and cause the change of the intensity of the XRD modulation peaks,[11] and may cause unprecise values for diffusion constants. Meanwhile, little is known about the relation between the solid-state amorphization and interdiffusion, and without the knowledge it is impossible either to predict or to control the SSIR in a rational manner.[19]

In this paper, a systematic investigation of interdiffusion phenomena in representative M-M and M-Si ML's is carried

 ©1999 The American Physical Society

out by the *in situ* low-angle XRD technique, and this method can measure the intensity of the modulation peak accurately and discriminate the effect of interfacial reactions, precipitation, and crystallization on the intensity in reactive ML's. The pure interdiffusion process can be achieved for those ML's by suitable deposition of the samples and monitored by the *in situ* XRD technique. This paper does not only increase the data based on reliable measurements, but also finds some diffusion characteristics in the ML's. The obtained interdiffusion data are compared to the literature data available for ML's, amorphous alloys, and to data for comparable crystalline solid. It is noted that fewer interdiffusion investigations have been made to compare the discrepancies between the M-M and metal-metalloid ML systems. In present studies, a comparison to the diffusion characteristic of the two types of ML's is presented, and such systematic investigations are necessary for formulating the general diffusion features and mechanism in ML's. The interdiffusion characteristics in the ML's are interpreted by the extended defect-controlled, interstitial-like diffusion mechanism, and the basic diffusion step involves a collective motion of a group of atoms. The relation between the interdiffusion and SSIR in the reactive ML's is also discussed.

II. EXPERIMENT

A. Sample preparation

Nanometer-scale compositional-modulated ML's were prepared by ion-beam sputtering from alternating elemental targets in a chamber with a base pressure of 1×10^{-7} Torr. Single-crystal Si (100) wafers were used as substrates and cooled by water through a substrate holder. The samples were sputtered in pure Ar atmosphere under pressure of 8×10^{-4} Torr. The total thickness of the films was about 0.8 μm. The modulation period (L) of the ML's ranges from 2 to 10 nm (L is the sum of thickness of the two sublayers). There are more than 100 modulation periods for the investigated ML's. An amorphous Si layer, about 10 nm in thickness, was capped onto the surface of the sample to avoid oxidation during the subsequent anneals. Details of the sample preparation were described at length in previous publications.[21–23]

It is found that the compositional modulation ML passes through two distinct processes depending on the annealing temperature range: a pure interdiffusion process and a solid-state reaction process. The interdiffusion process precedes the SSIR during anneals. This was confirmed by a high-angle XRD combined with a high-resolution transmission-electron microscope (HRTEM) observation. This phenomenon has also been found in other literature.[11] Figure 1 contains representative XRD curves of Ni-Si ML at various annealing processes and the schematic diagram of the Ni composition distribution in the ML in different annealing processes. As a result of initial intermixing in the deposition process, the amorphous Ni-Si multilayer consists of a Ni-rich amorphous-silicide sublayer with a small concentration of Si and Si-rich amorphous-silicide sublayer with a small concentration of Ni. The modulation structure was obtained by continuing deposition during the target-alteration process. The modulation structure of other as-deposited ML's is similar with that of Ni-Si ML. The annealing process from 423 to 613 K is a pure interdiffusion process for Ni-Si ML's and the annealing

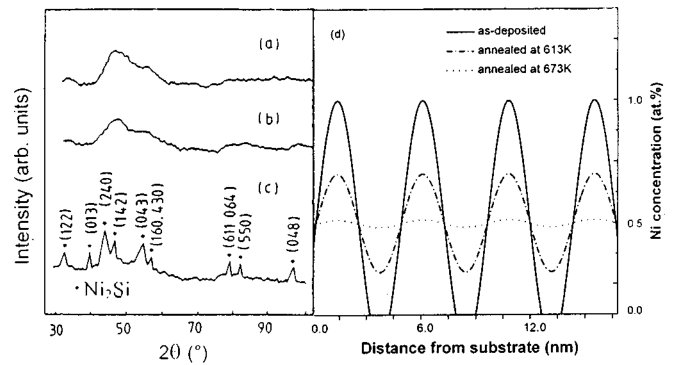

FIG. 1. High-angle x-ray diffraction pattern of the amorphous Ni-Si ML with $L=4.8$ nm and total thickness 0.8 μm. (a) as-deposited state; (b) annealing at 613 K; (c) annealing at 673 K; (d) schematic profile of the Ni concentration for the as-deposited state, annealed at 613 K, and annealed at 473 K of Ni-Si ML, respectively. The decrease of the amplitude of the Ni concentration curve is an indication of interdiffusion in the ML's.

leads to only homogenization of the modulation composition gradient as shown in Fig. 2(d). This result has also been confirmed by transmission electron microscope (TEM) observation.[15,21] Above 673 K, the process is due to SSIR resulting in the Ni_2Si formation. The interdiffusivities of these ML's are measured in the temperature range associated with pure interdiffusion.

B. Low angle x-ray scattering

The modulation structure and the microstructure of the ML were examined using AES [performed in a PHI-610 AES], low-angle XRD and HRTEM. All of the investigated as-deposited ML's have good modulation structure.[24,25] As a representative example, the AES depth profile from the as-deposited Fe-Ti ML is shown in Fig. 2. It exhibits a good compositional modulation structure with a shorter modulation period $L=2.0$ nm. The modulation period L was deter-

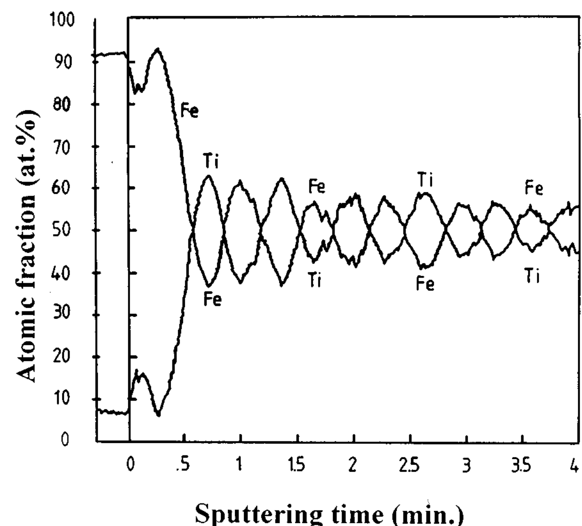

FIG. 2. Auger depth profile of Fe-Ti multilayer with $L=2.0$ nm. The composition of the ML is 50 at% Fe. The Auger spectrum shows the good composition modulation structure of the nanometer scale ML.

TABLE I. The modulated structural and compositional data for the investigated ML's. N is the number of the XRD modulation peaks. The total thickness of the ML's is about 0.8 μm. There are more than 100 modulation periods for each investigated ML.

System	L(nm)	Composition (at. %)	N
Fe-Ti	2.0	50.0 Fe	2
	9.0	51.5 Fe	5
Ag-Bi	9.0	45.0 Ag	4
Fe-Mo	2.74	50.0 Fe	2
Mo-Si	2.6	35.0 Mo	2
Ni-Si	4.8	49.2 Ni	2
Nb-Si	3.2	50.0 Nb	2
Ag-Si	6.7	43.0 Ag	4

mined using low-angle XRD and confirmed by HRTEM. A composition modulation structure, just like the Bragg lattice, gives rise to Bragg reflections or modulation peaks at the low-angle region ($0° < 2\theta < 15°$) in the XRD pattern. The value of L should be derived by using a modified Bragg's law, which takes into account the real part of the deviation δ of the refractive index from unity.[26] The modified Bragg law is:

$$\sin^2 \theta_n = \left(\frac{n\lambda}{2L}\right)^2 + 2\delta, \tag{1}$$

where n is the order of the XRD modulation peak, θ_n the diffraction angle of the nth order modulation peak, and λ the x-ray wavelength. The modulation periods of the ML's were accurately determined by using Eq. (1) and confirmed by cross-sectional HRTEM and other experimental techniques.[15,16,21–23] Table I presents the modulated-structural data for these ML's.

The *in situ* x-ray diffraction was performed on a Rigaku PSPC/MDG diffractometer with Cu K_α radiation. The diffracted x-ray was detected by a positional-sensitive proportional counter (PSPC) in 2θ angle range 0–150°. The annealing process was performed in pure Ar atmosphere. The Ar gas protection and a-Si cap layer were found to be effective in blocking gaseous impurities from entering the films during the annealing process. AES depth profiles from the as-deposited and the annealed samples show that the oxygen effect is below the detection limit. *In situ* technique together with PSPC can successively measure the intensity of the modulation peak under identical diffraction conditions for the same sample over the whole annealing period. In this way the intensity measuremental error is minimized. This is critical for intensity measurement, as small variations in sample position and alignment lead to large intensity changes in the modulation peaks. The uncertainty in the measurement of intensity of the modulation peak was estimated by measuring the same modulation peak several times without annealing between measurements. The maximum of the uncertainty for the intensity measurements is about 5%. The phase transition that may be caused by annealing in the ML is monitored simultaneously by high-angle XRD in the measuremental process, thus the interdiffusion investigations at pure interdiffusion process of the sample are guaranteed.

III. DIFFUSION THEORY

Interdiffusion in ML's can be determined from the rate of homogenization of compositional modulation structure of the ML's. According to the theory developed by Cahn and Hilliard,[25,26] a correction must be applied to Fick's law for compositionally inhomogeneous systems. In the one-dimensional case it is

$$\frac{\partial c}{\partial t} = D\frac{\partial^2 c}{\partial x^2} - \frac{2D}{f''}\kappa\frac{\partial^4 c}{\partial x^4}, \tag{2}$$

where D is the bulk interdiffusivity, c the atomic fraction of the components in position x at time t, f'' is the second derivative of the Helmholtz-free energy, and κ is the gradient-energy coefficient. For a composition modulation of small amplitude D, f'' and κ are independent of composition. Under these conditions a particular solution to Eq. (2) is

$$c = \exp\left[-D\beta^2\left(1 + \frac{2\kappa\beta^2}{f''}\right)t\right]\cos\beta x, \tag{3}$$

where $\beta = 2\pi/L$ is the wave number of the composition wave. In fact, in highly interdiffused ML's, an approximately cosinusoidal composition modulation can be obtained during the as-deposited process. The effective interdiffusivity is given by

$$D_e = D\left(1 + \frac{2\kappa\beta^2}{f''}\right). \tag{4}$$

The intensity I of the first-order low-angle x-ray modulation peak is proportional to the square of amplitude of the first Fourier component of the modulation composition[25] and depends on the effective interdiffusivity D_e of the ML's. By assuming that the linear decay of the first-order modulation peak represents the process in the isconfigurational condition, in the kinematic diffraction approximation, the decay of the $I(t)$ is related to the effective interdiffusion coefficient by[7]

$$D_e = \frac{-L^2}{8\pi^2}\frac{d}{dt}\ln\left[\frac{I(t)}{I(0)}\right]. \tag{5}$$

The logarithm of the intensity of the modulation peak was plotted against the annealing time. The interdiffusion coefficients were determined from the slopes of the straight fits versus annealing time. Thus, it is critical for the measurements of D_e to minimize the intensity error in the annealing process.

IV. RESULTS AND DISCUSSION

A. Application to metal-metal multilayers

The x-ray interference peaks due to the compositionally modulated structure are observed for all the investigated ML's in this paper. For Fe-Ti ML with $L = 9.0$ nm, the XRD modulation peaks up to the 5th order have been observed.

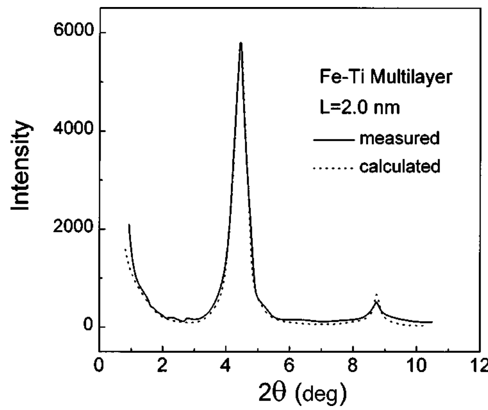

FIG. 3. Low-angle x-ray diffraction pattern (Cu K_α radiation) of the as-sputtered Fe-Ti multilayer with $L=2.0\,\mathrm{nm}$. The low-angle peaks indicate a composition modulation along the growth direction. The dash line is a fit to the low-angle x-ray spectrum based on the dynamical scattering theory. This specimen is used in the subsequent annealing and the interdiffusion coefficients are obtained from the decay of the first modulation peak during the isothermal annealing process.

The number of the XRD modulation peaks for each studied ML is given in Table I. As an example, the low-angle XRD pattern of the as-deposited Fe-Ti ML ($L=2.0\,\mathrm{nm}$) is shown in Fig. 3. The ML has a sharp modulation peak at $2\theta=4.44°$ and a weak peak at $2\theta=8.74°$. In the aim to evaluate the modulation structure and interface roughness σ. [The interface roughness is the degree of the structural imperfections at the interfaces induced by the intermixing during the deposition process or by the structural misfit of the sublayers] of the ML, a fit to the low-angle x-ray spectrum based on the dynamical scattering theory[27] and the roughness model of Nevot and Croce[28] has been done to provide information about the interface roughness and modulation structure. The dotted line in Fig. 3 represents the simulation pattern calculated for the rectangular composition profile. Clearly, the measured pattern is in good agreement with the calculated one. The measured angular position of the modulation peaks accurately coincides with the calculated one. According to the fit, the roughness of the inner interfaces for Fe-Ti ML's is 0.8 nm. The measured peaks are weaker and broader than the calculated one, and the difference is due to the structural imperfection such as variation in period, composition gradients, and intermixing during the deposition process at the interfaces.[29–31] Despite considerable imperfection, a good composition modulation along the film-growth direction is maintained in the studied ML's as evidenced by the x-ray spectra fit, AES depth profile, and cross-sectional TEM.[23]

Figure 4 represents a typical plot of the logarithm of the normalized intensity of the first modulation peak versus time at various annealing temperatures. No evidence for phase transition was detected by either XRD or TEM during the annealing processes in the Fe-Ti ML. This indicates the investigations were made in the pure interdiffusion stage. A feature is worth noticing from the plot; the intensity exhibits a more rapid nonexponential decay in the early stage of the annealing (0–1.0 h). This type of behavior has also been generally found for many other ML's in the literature.[4,7,12,17,18] The enhancement in intensity decay is contributed to the annihilation of the large number of nonequilibrium defects and homogenization of the steep composition gradient in the as-deposited multilayers at the earlier annealing stage. A relative steady exponential decay state was obtained after 1.0 h annealing. The accuracy of Eq. (5) for obtaining the interdiffusivity is strongly limited by the nonequilibrium defects, and especially, the steep composition gradient that exist in the early stage of the annealing.[7] The effective interdiffusivities were determined by the linear fit from the linear part in Fig. 4. At 458 K, $D_e(458\,\mathrm{K})=1.085\times10^{-25}\,\mathrm{m^2/s}$. Raising the temperature to 498 K the slope increases, indicating the temperature dependence of the interdiffusivity. The effective interdiffusivities at various annealing temperatures can be summarized in the Arrhenius

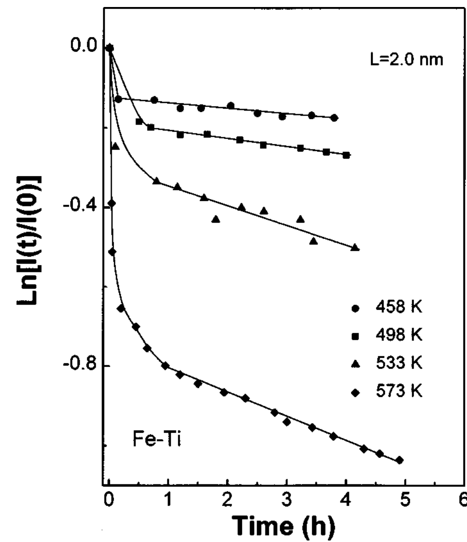

FIG. 4. Decay of the intensity of the first-order modulation peak of Fe-Ti multilayer. ($L=2.0\,\mathrm{nm}$) as a function of annealing time at various annealing temperatures. A more rapid nonexponential decay in the early stage of the annealing (0–1.0 h) is contributed to the annihilation of the large number of nonequilibrium defects and homogenization of the steep composition gradient in the as-deposited multilayers at the earlier annealing stage. The interdiffusivities were obtained from the linear region occurring in the later part of the annealing process, where the local equilibrium has been reached.

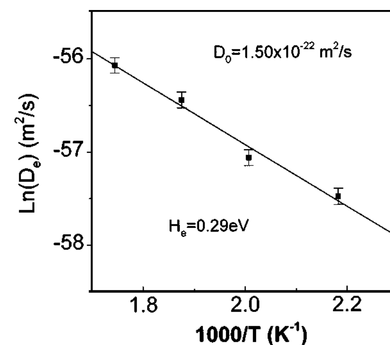

FIG. 5. Temperature dependence of the interdiffusivity D_e for Fe-Ti ML. The solid line is the linear fit of the diffusion data. The fit indicates that the interdiffusion data display excellent Arrhenius behavior. The activation energy H_e and preexponential factor D_0 are obtained from the fit.

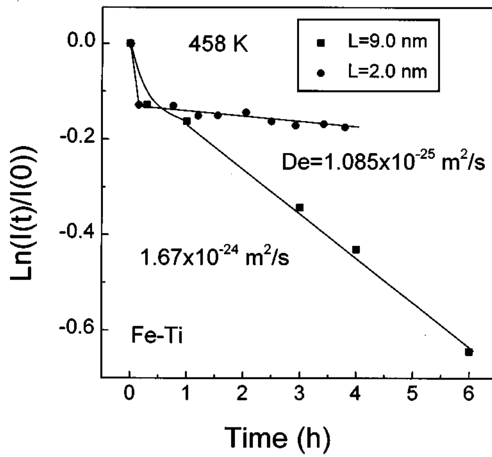

FIG. 6. Decay of intensity of the first modulation peak for the Fe-Ti ML's with $L=2.0$ and 9.0 nm, respectively. The decay of the intensity of the ML with larger L is faster than that of the ML with smaller L, indicating the L dependent of the interdiffusion in the ML's.

plot in Fig. 5. The diffusion data displays excellent Arrhenius behavior. From the Arrhenius expression $D_e = D_0 \exp(-H_e/k_B T)$, the activation energy H_e and preexponential factor D_0 can be obtained from a plot of D_e versus $1000/T$. The effective interdiffusivities are expressed as $D_e = 1.50\times 10^{-22}\exp(-0.29/k_B T)$ [m^2/s], (458–573 K). k_B is the Boltzmann constant. Figure 6 shows the decays of $I(t)$ for Fe-Ti ML's with different modulation periods annealed at 458 K. The intensity attenuation curves of Fe-Ti ML with $L=9.0$ nm is much faster than that with $L=2.0$ nm. The effective interdiffusivities for the two samples with $L=9.0$ and 2.0 at 458 K are 1.67×10^{-24} m^2/s and 1.085×10^{-25} m^2/s, respectively. This result indicates that the effective interdiffusivity is modulation-period dependent in Fe-Ti ML's. The values of H_e and D_0 for Fe-Mo, Ag-Bi ML's (Ag-Bi ML with positive heat of mixing is a system where the SSIR is difficult to occur) are also obtained by using the *in situ* XRD method. The results are listed in Table II.

B. Application to metal Si multilayers

The interdiffusion in the Mo-Si, Ni-Si, Nb-Si, and Ag-Si ML's are investigated by the *in situ* XRD method. The effective interdiffusivities for these metal-Si ML's can also be summarized in the Arrhenius plot, and the obtained values of D_e and H_e are listed in Table II. The obtained interdiffusion data for Mo-Si ML are in accord with the report of Ref. 32. For the interdiffusion in the Ni-Si ML, the obtained results are agreement with those estimated from the studies of the growth kinetic of NiSi precipitates in a-Si,[33] as well as from investigation of the diffusion of Ni in amorphous Si by secondary ion-mass spectrometry and RBS.[34]

TABLE II. The interdiffusion parameters of the studied ML's, $\Delta r/r$ is the atomic-radius difference of the constituents in the ML.

System	$\Delta r/r$(%)	H_e (eV)	D_0 (m^2/s)
Ag-Bi	16.5	0.21	4.30×10^{-21}
Fe-Ti	14.0	0.29	1.50×10^{-22}
Fe-Mo	9.8	0.33	2.13×10^{-21}
Mo-Si	5.2	0.37	6.20×10^{-21}
Ni-Si	6.2	0.69	2.13×10^{-17}
Ag-Si	8.7	0.24	2.02×10^{-20}
Nb-Si	10.1	0.55	2.20×10^{-18}

C. Validity of the *in situ* XRD interdiffusion measurements

There is a key test by which to determine whether a method can be used to correctly measure the interdiffusivity in solid, that is, the obtained interdiffusivities as a function of temperature should be described by the Arrhenius relation.[35,36] The diffusion data from our experiments for various systems display excellent Arrhenius behavior. The consisted Arrhenius behavior of D_e suggests that the *in situ* XRD is the most sensitive method available to probe interdiffusion information of the ML's with nanometer scaled L at low temperatures. This was also verified by a series of other studies.[10–18] The values of D_e for above ML's are quite low (10^{-23}–10^{-25} m^2/s) compared with the extrapolation of the published high-temperature diffusion data in bulk alloys metals,[37] and crystalline silicon.[38] However, they are similar to those reported in many other ML's (Refs. 7, 17, and 18) and amorphous alloys.[39–42] The interdiffusion behavior in the ML's is characterized by two parameters, the preexponential factor D_0 and the activation energy H_e. The interdiffusion parameters obtained in this paper are summarized in Table II. To see any distinct difference in ML's D_0 and H_e in the ML's are compared to other amorphous and crystalline solids and shown in Table III. The obtained values of D_0(10^{-17}–10^{-22} m^2/s) are much smaller than the typical values of that in crystalline materials (10^{-5}–10^{-7} m^2/s), and the differences are more than ten orders of magnitude. The values of D_0 for liquid metal and amorphous alloys are normally much smaller than that of corresponding crystalline materials. The feature of D_0 in the ML's is similar to that of liquid metals and amorphous alloys.[7,47] The feature can hardly be attributed to the routine of experimental errors, and is related to the peculiar diffusion mechanism in the ML's. We will discuss this in detail in Sec. IV E.

The values of H_e obtained in ML's are quite small (<1.0 eV). Our results are similar to that of the interstitial diffusions and/or interstitial-like diffusions in other solids as shown in Table III. It is well know that the small values of D_0 and H_e are a general feature of interstitial diffusers in crystalline solid [e.g., transition metals diffusion in α-Zr,[48] crystalline Si(c-Si) (Ref. 49)]. The small values of D_0 and H_e are even a general feature for interstitial-like diffusers in amorphous solid [e.g., a-Si, amorphous alloys (a-alloys)]. In comparison, the noninterstitial diffusers in both crystalline and amorphous solids shown in Table III [e.g., Si(Ni) diffuse in c-Si(c-Ni) by monovacancy mechanism, for Si diffusion in c-Si in the range of 1493–1623 K, D_0 and H_e 1.80×10^{-1} m^2/s and 4.68 eV, respectively] have larger H_e, and the values of D_0 are several orders in magnitude larger than that of interstitial diffusion. The discrepancy is attributed to the diffusion mechanism difference among these solids. The D_0 and H_e are determined by the interdiffusion mechanism and the change of the diffusion mechanism will

TABLE III. A summary of the D_0, He, and diffusion mechanism for various *a*-alloys and crystalline solids. *c*-Si, *c*-Ni are crystalline Si and Ni, respectively, a-$Ni_{50}Zr_{50}$ represents the amorphous $Ni_{50}Zr_{50}$ alloy. In the diffusion-mechanism column, *a* stands for the interstitial diffusion mechanism, *b* stands for the noninterstitial diffusion mechanism, and *c* for the interstitial-like diffusion mechanism.

System	Diffusion mechanism	D_0 (m^2/s)	H_e (eV)	Refs.
Ni in *c*-Si	*a*	1.79×10^{-7}	0.47	38
Ni in *c*-Ni	*b*	5.0×10^{-5}	2.83	44
Si in *c*-Si	*b*	1.8×10^{-1}	4.68	44
Ni in a-$Ni_{50}Zr_{50}$	*c*	1.7×10^{-7}	1.4	45
Fe in a-$Fe_{91}Zr_9$	*c*	3.1×10^{-7}	1.45	46
Zr in a-$Fe_{91}Zr_9$	*b*	2.1×10^{-3}	2.41	46
Fe in *c*-Si	*a*	1.3×10^{-7}	0.68	49
Fe in a-$Fe_{40}Ni_{40}B_{20}$	*b*	6.8×10^{-3}	2.39	40
Co in a-$Ni_{50}Zr_{50}$	*c*	3.7×10^{-7}	1.35	44
Co in *c*-Si	*a*	9.0×10^{-8}	0.37	49
Co in a-$Co_{89}Zr_{11}$	*c*	8.2×10^{-7}	1.47	42
Au in a-$Co_{89}Zr_{11}$	*b*	7.9×10^{-1}	2.74	42
Cu in *c*-Si	*a*	4.7×10^{-7}	0.43	49
Cu in *a*-Si	*c*	5.0×10^{-11}	1.2	43
Ag in a-$Cu_{50}Zr_{50}$	*c*	1.3×10^{-15}	0.72	60
Au in a-$Cu_{50}Zr_{50}$	*c*	1.7×10^{-7}	1.55	60
Bi in a-$Pd_{78}Cu_{16}Si_6$	*b*		3.69	39
Pt in a-$Pd_{78}Cu_{16}Si_6$	*c*		1.39	39

show up in different features of the parameters. Based on the above analysis, the similarity between the interdiffusion in the ML's and interstitial or interstitial-like diffusion in other solids, permit the hypothesis: the interdiffusion in M-M and M-Si ML's may be governed by an interstitial-like mechanism. However, the microstructure of the ML's with high-density interfaces are not thermodynamic stable. Slight variations of the preparation parameters during the deposition process like the deposition rate and the substrate temperature lead to high strain and a large number of nonequilibrium defects in the ML's. The strain and defects in the ML's must affect the interdiffusion. The high-density nonequilibrium defects in the ML's could act as a fast diffusion path[50] and reduce D_e and H_e. Strain frequently exists in the high-density interfacial ML's because of the thermal expansion mismatch with the substrate and coherency strains between the sublayers. Even the strains can be relaxed by annealing. They were found to remain at least partially throughout the whole interdiffusion.[13] The strains may cause easing passage of the interstitial diffusers through another sublayer and also reduce H_e.

D. Correlation between the atomic-size difference and interdiffusion in the ML's

As shown in Fig. 6, the D_e is L dependent in the Fe-Ti ML. In fact, this is a general feature resulting from the large chemical-potential gradient in compositional modulated ML's.[13,25,26,32,51] To compare the interdiffusion behavior in various ML's the bulk interdiffusivity, therefore, should be

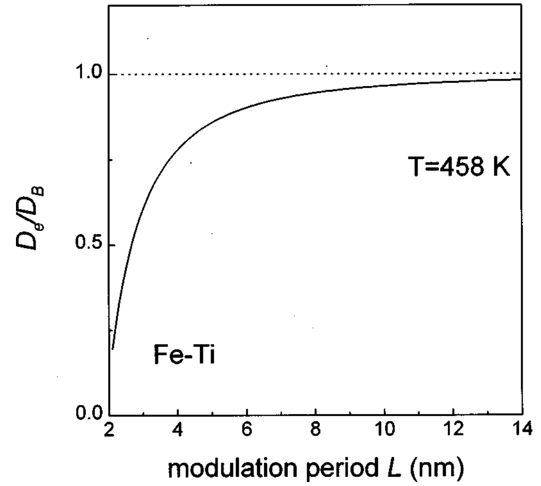

FIG. 7. The relation between D_e/D_B and L for Fe-Ti ML at 458 K. The effective interdiffusivities dependence of L is significant for ML's with smaller L, when L is larger than 10 nm, $D_e \approx D_B$.

estimated. According to Cahn's theory,[25,26] the relation between effective interdiffusivity and bulk interdiffusivity D_B is given by

$$D_e = D_B\left(1 + \frac{8\pi^2\kappa}{f''}\frac{1}{L^2}\right). \tag{6}$$

Assuming a regular solution model for the ML's as discussed by Greer and Spaepen,[7] κ and f'' are given by

$$\kappa/f'' = \frac{\Delta H_m r^2}{6(RT - 2\Delta H_m)}, \tag{7}$$

where ΔH_m is the enthalpy of mixing of a system at the equiatomic composition, and r is the interactomic distance. Substituting standard values[52] for these variables, one obtains the values of κ, f'', and κ/f'', and then the bulk interdiffusivity D_B. For Fe-Ti ML at 458 K, $\kappa = -4.1\times10^{-10}$ J/m, $f'' = 9.2\times10^9$ J/m^3, $\kappa/f'' = -4.5\times10^{-20}$ m^2, and $D_B = 1.75\times10^{-24}$ m^2/s. Figure 7 shows the quotient D_e/D_B dependent of L for Fe-Ti ML at 458 K. It can be seen that the D_e dependence of L^{-2} is significant for ML's with L less than 10 nm. When L is larger than 10 nm, $D_e \approx D_B$. The obtained values of κ/f'' and D_B for other ML's are listed in Table IV.

Figure 8 displays the D_B and H_e of the M-M ML's versus the atomic radius difference of the constituents $\Delta r/r$ in the ML's, where $\Delta r = r_A - r_B$, $r = (r_A + r_B)/2$, and r_A, r_B are the atomic radius of the two constituents of the ML, respectively. The lines were drawn visually. It is seen that D_B and H_e show a correlation with the atomic size difference for the M-M ML's. The ML with larger atomic-size difference exhibits faster interdiffusion and lower activation energy. This indicates that an atomic-size difference dependence of D_B exists in the M-M ML's. The interdiffusion data of the Pt-Co ML in Ref. 13 follows the trend as shown in Fig. 8. However, the data of D_B and H_e scatter so much that there is no correlation between D_B and $\Delta r/r$ in the M-Si ML's, as shown in Fig. 9. The size dependence of diffusion coefficients and H_e were found to be the general features of the

TABLE IV. The calculated values of κ, f'', κ/f'', and bulk interdiffusivity D for various ML's studied in this paper and Pt-Co ML in literature (Ref. 13) at 458 K. $\Delta r/r$ is the atomic-radius difference of the constituents in the ML.

ML's	$\Delta r/r$ (%)	κ/f'' (10^{-22} m^2)	D_B (m^2/s)
Fe-Mo	9.8	−38.0	4.1×10^{-25}
Pt-Co	10.6	−78.2	3.4×10^{-25}
Fe-Ti	14	−450.0	1.75×10^{-24}
Ag-Bi	16.5	0.0035	2.0×10^{-23}
Mo-Si	5.2	−100	5.2×10^{-25}
Ni-Si	6.2	−67.1	4.12×10^{-24}
Ag-Si	8.7	−65.1	8.22×10^{-24}
Nb-Si	10.1	−124.8	2.68×10^{-24}

metal diffusion in M-M a-alloys, crystalline α-Ti, and α-Zr.[40,48,53,54] This correlation is interpreted qualitatively as being caused by different elastic distortions of the matrix during the thermal-activated jump of the differently sized atom.[53] A number of exceptions in the case of metal-metalloid a-alloys have also been found.[53,55] The similarities of the structural dependence between interdiffusion in the ML's and a-alloys also indicate there is the similarity in the diffusion mechanism between the two systems. The atomic-size difference in the ML's is an important effect on the interdiffusion in ML's, but it is only one of several factors effecting the interdiffusion. The other factors are the configuration of the constituents and chemical factor. An obvious size difference dependent can be observed only if other factors are negligible compared to the structural factor. It seems that the structural effect in the studied M-Si ML's are less important compared with the M-M type ML's.

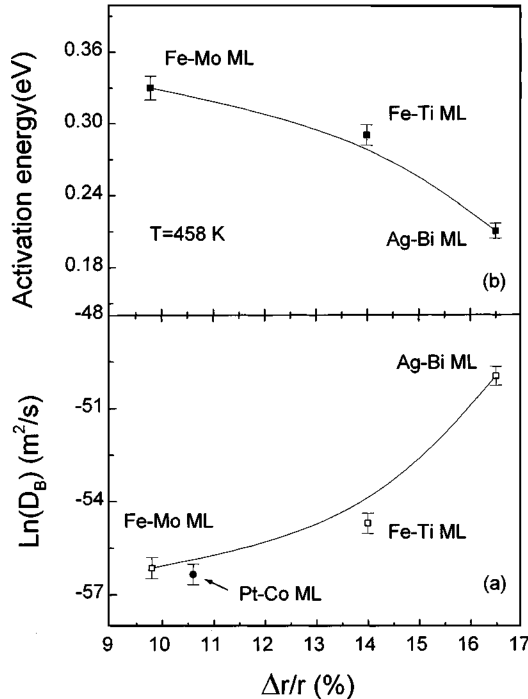

FIG. 8. The bulk interdiffusivity D_B of the metal-metal ML's vs the atomic-radius difference in the ML's. $\Delta r = r_A - r_B$, $r = (r_A + r_B)/2$, r_A, and r_B are the atomic radius of the two constituents of the ML, respectively. The line was drawn visually. D_B and H_e show a correlation with the atomic-size difference for the M-M ML's.

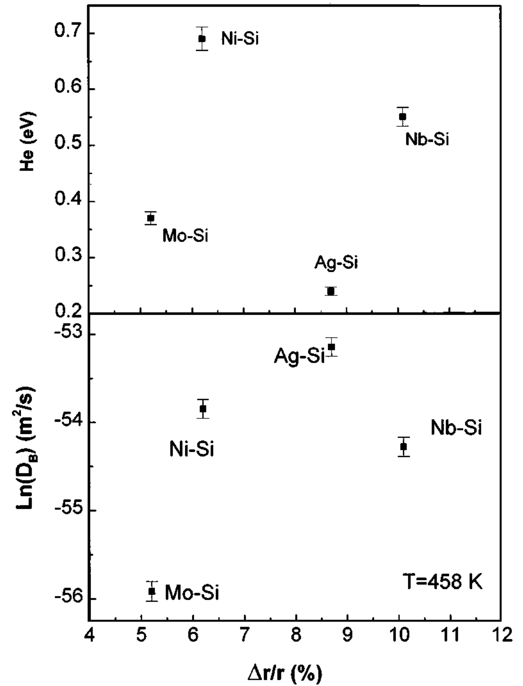

FIG. 9. The bulk interdiffusivity D_B of the metal-Si ML's vs the atomic-radius difference in the ML's. The data of D_B and H_e scatter so much that there is no correlation between D_B and $\Delta r/r$ in the M-Si ML's.

It is found from a comparison of the interdiffusion in Table II that the activation energies are lower in the M-M ML's than in the M-Si ML's. This may also result from the size difference between the two types of ML's. As is shown in Table II, M-Si ML's have a relatively larger atomic-size difference than that of the metallic constituents in the M-M ML's. We note that in the investigations of diffusion the energy barrier for the same migrating species is generally smaller in the M-M-type than in the M-Si-type a-alloys, and the discrepancy has been correlated with the known size difference between the M-M and M-Si a-alloys.[56] As shown in Table II, there is a basic size difference between the M-M and M-Si ML's. M-M-type ML's, in which the constituents have a larger atomic-size difference than that of M-Si ML's, have a larger mismatch strain, and then results in the relative lower value of H_e in M-M ML's.

E. Proposal for interdiffusion mechanism in the reactive ML's

An empirical correlation between D_0 and H_e has been observed and is known as the isokinetic relation in amorphous and crystalline alloys,[57]

$$\ln D_0 = \ln A + H_e/B, \tag{8}$$

which is expected to fulfill with specific parameter A and B for a whole set of diffusion coefficients if they are based on a common diffusion mechanism. A plot of $\ln D_0$ and H_e for the interdiffusion data in this paper is presented in Fig. 10. The diffusion data reported in Zr-based a-alloys,[37] crystalline

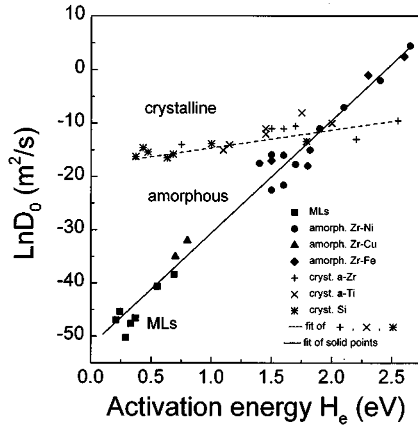

FIG. 10. The plot of LnD_0 and H_e for the ML's Zr-based a-alloys (Ref. 37) and crystalline α-Zr, α-Ti (Ref. 54), and Si (Ref. 49). The solid and dash lines are linear fit of the diffusion parameters for the ML's and Zr-based a-alloys. The parameters A and B obtained from the fit for the ML's and Zr-based a-alloys are obviously correlated according to the relation $\ln D_0 = \ln A + H_e/B$ with the values of A and B as $9.85\times 10^{-21}\, \mathrm{m^2/s}$ and 0.053 eV, respectively. The value of A ($1.6\times 10^{-7}\, \mathrm{m^2/s}$) and B (0.37 eV) for crystalline α-Zr, α-Ti, and Si are quite different from those of a-alloys and ML's.

α-Zr, α-Ti,[54] and c-Si (Ref. 49) are also given in the figure to see any distinct difference from the interdiffusion in the ML's. In spite of the relative large scatter, the diffusion parameters for the ML's and Zr-based a-alloys are obviously correlated according to Eq. (8) with the values of A and B as $9.85\times 10^{-2}\, \mathrm{m^2/s}$ and 0.053 eV, respectively. The parameters A and B are almost the same within the experimental error as reported for other a-alloys.[40,53,58,59,60] The value of A ($1.6\times 10^{-7}\, \mathrm{m^2/s}$) and B (0.37 eV) in crystalline α-Zr, α-Ti, and Si are quite different from those of a-alloys and ML's, which means the different interstitial diffusion behaviors between the crystalline α-Zr, α-Ti, Si, and ML's. The observed isokinetic relation between a-alloys and ML's further confirms that a similar diffusion mechanism is operating in ML's and a-alloys. In fact, just like a-alloys, the ML's with a high density of interface and a large number of nonequilibrium defects are in the metastable state, and they contain a large number of nonequilibrium defects. Combining with the analysis in Sec. IV C, it can be concluded that the similarity in diffusion behavior between the ML's and a-alloys is reasonable. The diffusion, unlike in crystalline α-Zr, α-Ti, and Si, is strongly affected by defects in the ML's. The defects in the ML may act as trapping centers, and trap diffuser atoms temporarily and make the atoms undergo a trap-retarded diffusion, reducing the interdiffusivity by[61] $D_e = D_f/[I + C_t \exp(H_t/k_B T)]$, where D_f is the interstitial diffusivity in hypothetical trapping-free ML's C_t and H_t are the atomic fraction of traps and the binding enthalpy, respectively. The decrease of D_e in ML's results from the diffuser having to pass through the trapping centers in ML's.

From Fig. 10, one can see that the values of D_0 and H_e in the ML's are smaller in several orders of magnitude than the a-alloys, even though they correlate according to Eq. (8). It is known that D_0 cannot be determined as accurately as the activation energy in the diffusion measurements; the small difference in D_0 of even as much as an order of magnitude is not of major concern. In this case, however, the differences are found to be more than ten orders of magnitude. Such differences can hardly be attributed to experimental errors. This diffusion characteristic was considered to result from the preexisting nonequilibrium defects in the ML's with a shorter value of L.[7,32] D_0 is related to defect by $D_0 = D_0^f/C_t\alpha$,[48,43] where D_0^f is the preexponential factor in a hypothetical defect-free ML, α the parameter related to the binding entropy, the attempt frequency for an diffuser atom, and the number of defect sits available around a defect. The difference of C_t between crystal Si (0.1 ppm%) and amorphous Si (<1%) formed by deposition is in the order of 10^7. So, the difference of C_t between a hypothetical defect-free ML and the studied ML should be less than 10^7. Therefore, the significant difference in D_0 cannot be totally attributed to the fraction of the defect in ML's. To interpret the results, we pay particular attention to D_0, which displays a significant difference among the crystalline solids, a-alloys, and ML's. Interdiffusion is governed largely by the local structural environment and defects. With regard to long-range diffusion, the purely geometrical part of the disorder in the ML's can be discarded due to the quite well short-range order; the local microstructure in ML is close to that of crystalline solids. For example, in M-Si ML's, the a-Si and c-Si are similar in local atomic microstructure.[62] However, the defects in the ML's must be different from that in crystalline solids, because the D_0 and H_e for the interdiffusion in ML's are extremely small. An extended nonequilibrium defect may be responsible for the interdiffusion in the unstable ML's structures. The extended defect is complex and involved a large number of neighboring atoms, rather than the interstitial site or monovacancy, which have been shown to govern the diffusion in crystalline. The conclusion is discussed in detail below. It is known that D_0 can be written as[63]

$$D_0 = a^2 c f \nu_0 \exp\left(\frac{\Delta S}{k_B}\right), \tag{9}$$

where a is the mean-jump distance, c the geometric factor, f the correlation factor, ν_0 the jump-attempt frequency, and ΔS the change in the activation entropy during the jump process. D_0 is determined by the five terms. The significant D_0 differences of more than ten orders of magnitude between crystalline solids and ML's must result from the large changes in these terms. Since the local microstructures are similar between the crystalline solids and ML's, the constant c, which is geometric in origin, and the mean-jump distance a could not be significantly different between the crystalline solids and ML's. For any reasonable diffusion mechanism and structure, f would vary between five to ten at most. The small changes of the three terms cannot account for the D_0 differences between crystalline solids and ML's. The jump-attempt frequency ν_0, usually taken to be the order of the Debye frequency in crystal, is 10^{13}/s. In the a-alloy, ν_0 was observed to be in the order of 10^9/s.[64] The values of ν_0 would be roughly in the same order of magnitude as that of the a-alloys, and the difference is about four orders of magnitude. Thus, the large differences between D_0's in crystalline solid and ML's would be attributed to the entropy term

TABLE V. The results of solid-state interfacial reaction in the ML's. X is the crystalline compound.

ML's	D_B (m^2/s)	Reaction results
Fe-Mo	4.1×10^{-25}	
Fe-Ti	1.75×10^{-24}	Amorphous
Ag-Bi	2.0×10^{-23}	
Mo-Si	5.2×10^{-25}	X
Ni-Si	4.12×10^{-24}	Amorphous
Ag-Si	8.22×10^{-24}	Amorphous
Nb-Si	2.68×10^{-24}	Amorphous

$\exp(\Delta S/k_B)$, e.g., ΔS has to be large and negative. For diffusion in crystalline solids, ΔS is of $(3-5)k$, which corresponds to the single-atom diffuse with interstitialcy or monovacancy mechanism.[65] ΔS in ML's is estimated to be $-(8-15)k_B$.[66] The large and negative value of ΔS in the ML's indicate that the basic diffusion step in the ML's is not a single atom jumping into a vacancy or replacing an interstitial site in the case of diffusion in crystalline solids, but the collective motion of a group of atoms. The entropy of $-(8-15)k_B$ roughly corresponds to a cluster with 8 to 15 atoms, and the cluster may move in an interstitial way through the nonequilibrium extended defects, possibly like the free volume in liquid and *a*-alloys, which acts as diffusion path in the ML's. This suggestion is also consistent with the smaller H_e and the marked correlation between the D_0 and H_e found for interdiffusion in these ML's. The extremely small values of D_0 and H_e, displaying marked correlation, are generally taken as evidence of a collective atomic-diffusion mechanism in liquid and *a*-alloy. The jumps of clusters of atoms have been observed in the molecular dynamics studied of model glasses and a binary softsphere mixture near the glass transition. The jump seems to be closely related to the low-frequency excitations in glasses, and the groups of atoms are found to move in a caterpillar motion between two nearby equilibrium positions, corresponding to small activation energies. The collective atomic movements resemble the atomic relaxation motion in *a*-alloys.[60] Highly collective diffusion has also been suggested in liquid and *a*-alloys,[51,64] and there are several reasons to support the proposal of a collective mechanism in liquid, glasses, and *a*-alloys.[60] The ML's with a high density of interface and a large number of nonequilibrium defects are in the metastable state. The local microstructure in ML is close to that of *a*-alloys. The interdiffusion is governed mainly by the local microstructure and defects. Therefore, the similarity in diffusion behavior and mechanism between the ML's and *a*-alloys is reasonable.

F. Relation between interdiffusion and SSIR in ML's

SSIR's are widely found in M-M and M-Si ML's.[1] The SSIR results in the studied ML's are listed in Table V. The SSIR in ML's is clearly kinetically, as well as thermodynamically constrained. No SSIR were observed in Ag-Bi and Fe-Mo ML's, for they do not satisfy the thermodynamic and kinetic requirements of SSIR. Two general approaches to analyzing the kinetic constraint in SSIR are based on competitive-growth arguments[67,68] and nucleation,[21,69] respectively. Both of the approaches, however, have limited interpretation capabilities, due to their dependence on unknown kinetic constants of interfacial energy and the kinetic barriers. The SSIR can be better understood in terms of the interdiffusion behaviors pertinent to the ML's.

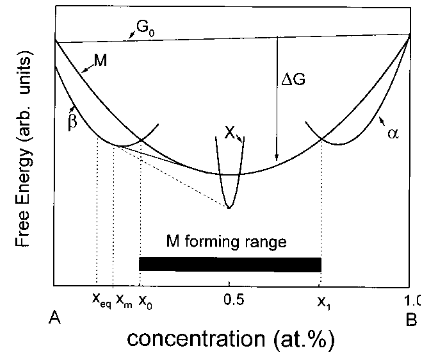

FIG. 11. A schematic plot of the free-energy curves for the as-deposited ML, G_0, A, and B solid solution in the form of crystalline phase α, β, respectively, a crystalline intermetallic X with narrow composition range, and an amorphous phase M with a broad composition range. ΔG is the driving force for the SSIR in the reactive ML. The figure exhibits schematically the SSIR trend of the reactive ML.

To clarify the relation between the interdiffusion and SSIR in the ML's, a schematic plot of the free-energies diagram for a ML consisting of pure elements A and B sublayers is illustrated in Fig. 11, which exhibits schematically the SSIR trend of the ML. The free-energy curves for the as-deposited ML, G_0, A, and B solid solution in the form of a crystalline phase α, β, respectively, a crystalline intermetallic X with a narrow composition range, and an amorphous phase, M, with a broad composition range are shown in the figure. This is the general case in the ML's with negative heat of mixing.[67] As illustrated in the diagram, ΔG is the driving force for the SSIR in the reactive ML, and the formation of X is favored in the view of energy point. However, consider the schematic diagram in Fig. 12, where the X or M embryo has formed in the interface between pure A and pure B sublayers. In this case, An atoms in X or M would lease X or M to diffuse into solution on the B sublayer, and B will leave X or M to go into solution on the A sublayer. This would happen until the A and B solution adjacent to the X or M embryo reached $x_{A,\mathrm{eq}}$ and $x_{B,\mathrm{eq}}$, or until X or M dissolved. Therefore, an embryo of X or M, regardless of its size, cannot

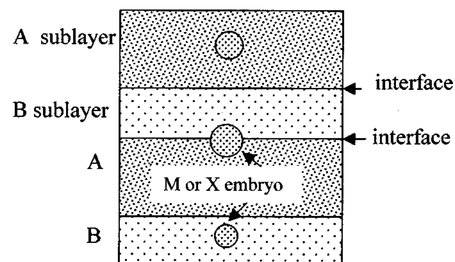

FIG. 12. A schematic illustration of crystalline particles X or amorphous particles M forming in a ML consisting of pure A and B sublayers.

nucleate and grow between pure A and B sublayers, even though the formation of X or M would reduce the energy of the ML systems. Similar analysis can demonstrate that X or M forms inside pure A or B sublayers as shown in Fig. 12 is also impossible. Therefore, interdiffusion is required before SSIR between pure sublayers. The interdiffusion must precede the nucleation of a phase induced by the SSIR in the ML's, because the nucleation and growth of a phase that involves a composition change requires diffusion of the constituent to form nuclei. The conclusion is consistent with the interdiffusion experimental results in the ML, which show that there is a pure interdiffusion process before the SSIR happens.

It is known that ML's with a strong SSIR trend display an interdiffusional asymmetric.[12] For example, the mobility of Ni in a-Si is faster than that of Si in Ni in the interdiffusion process of Ni-Si ML,[15] so that the interdiffusion is approximately equivalent to a single-diffusion process of the dominant diffuser in the Si sublayers. Let A atoms diffuse much faster in the β phase than B atoms diffuse in the α phase, and the interdiffusion is then considered as a single-diffusion process. In this case, as the interdiffusion proceeds with sufficiently low interdiffusivity, the X in β is the first possible forming phase when β reaches the composition $x_{A,\mathrm{eq}}$, as defined in Fig. 11. This kind of interfacial reaction has been observed in Mo-Si ML. In the Mo-Si ML, where the interdiffusion is very slow, the crystalline compound $MoSi_2$ is the first formation phase. If X does not nucleate and the interdiffusion continues, it will next become possible to nucleate M when a sufficient volume of β reaches x_M. Thus, the time required for nucleation of the X or M, e.g., the time required for interdiffusion to the point at which the X or M can nucleate and grow, controls the SSIR products. If neither the stable X nor the metastable amorphous phase nucleates, β eventually reaches the composition x_0, at which the solid solution becomes supersaturated and unstable with respect to M. As a consequence, β would transform polymorphically to M. It can be concluded that the SSIR in the ML's is constrained by the rate of interdiffusion and the rate of nucleation of the competitive phases. The appearance of the amorphization reaction in the ML's indicates that the nucleation of stable X is slow relative to interdiffusion and nucleation of an amorphous phase. The thermodynamic and kinetic factors were generally thought to govern the SSIR in the ML's.[67–69] In thermodynamics, the large negative heat of mixing provides the driving force for the SSIR. In kinetics, the energy barrier for the nucleation, which involves the interfacial energy, determines the SSIR phase selection, and the phase which has the higher nucleation rate or low-energy barrier is the favored forming phase in the interfacial reaction. From the above analysis, it is concluded that SSIR is controlled not only by the driving force and energy barrier for nucleation, but also by the interdiffusion rate in the ML's. Because the interdiffusion between the constituents is slow, it could be expected that unpolymorphic nucleation of X and M would be slow and the amorphization will be favored at composition above x_0 and below x_1 by polymorphic transformation. That is, the possibly amorphous forming composition range is $x_0<x<x_1$ as illustrated in Fig. 11. In fact, the amorphous phase induced by SSIR in the ML's does form in the center composition range in the diagram.[65] For example, for Ni/Si ML, the amorphous phase forms in the range 25–62 at Ni.[21] From these considerations, it can be seen that the interdiffusivities have the significant effect on the phase selection of the SSIR in the ML's.

V. SUMMARY AND CONCLUSIONS

The interdiffusion in metal-metal and metal-Si multilayers was studied by using an *in situ* low-angle XRD method. The pure interdiffusion process before the interfacial reactions in the ML's was clearly separated from the subsequent interfacial reactions by taking advantage of the unique compositionally modulated ML's and the *in situ* low-angle XRD method. The interdiffusivities were accurately measured in various ML's. The obtained values of D_e for the ML's are in the range of 10^{-23}–$10^{-25}\,\mathrm{m^2/s}$ and they are much lower compared with the extrapolation of the published high-temperature diffusion data in bulk alloys, pure metals, and crystalline silicon. However, they are similar to those reported in many other ML's and a-alloys. The obtained interdiffusion coefficients are temperature dependence and can be described by the Arrhenius relation. The values of the preexponential factor D_0 and activation energy H_e for interdiffusion in the M-M and M-Si ML's are much smaller than the impurity-diffusion coefficients in crystalline solids. The extremely small D_0 in the ML's is about the same order in magnitude as that of liquid metals and amorphous alloys. The values of the activation energy in the ML's are less than 1.0 eV, which are similar to that of the interstitial diffusions and/or interstitial-like diffusions in other solids. The interdiffusion coefficient data and the activation energy in the studied M-M ML's were found to correlate with the atomic-size difference between the constituents in the ML's. The interdiffusion parameters D_0 and H_e agree with an experimental correlation $\ln D_0 = \ln A + H_e/B$ that appears to be valid for diffusion in a-alloys and crystalline Zr, Ti, and Si.

A comparison of the interdiffusion parameters and behavior between the a-alloys and crystalline Si, α-Zr, and α-T suggests that the interdiffusion mechanism in the ML's is analogies with that in the a-alloys. The extremely small values of D_0 and the marked correlation between the D_0 and H_e for interdiffusion in ML's indicate that the interdiffusion may involve the jumping of clusters consisting of 8–15 atoms instead of the single-atom jump. These atoms collectively move in a complicated way between the extended nonequilibrium defects by thermal activation in the ML's.

It is demonstrated that the interdiffusion has close relations with the SSIR in the binary ML's, the interdiffusion must precede the interfacial reactions and occur before nucleation of any possible phase in the ML's. The preceded interdiffusion combining with the thermodynamic driving force and energy barrier for nucleation constraints the phase selection and favors the amorphous formation in polymorphic transition in SSIR of the ML's.

ACKNOWLEDGMENTS

We would like to thank Dr. M. X. Pan for his useful discussions and help. This paper was supported by the National Natural Science Foundation of China (Grant No. 59871059), and the Foundation of Chinese Space Agency for Young Scientists in High Technology (Grant No. 863-2.98.9).

*Author to whom correspondence should be addressed. Electronic address: whw@aphy.iphy.ac.cn

[1] B. M. Clemens and R. Sinclair (unpublished).

[2] *Physics, Fabrcation, and Applications of Multilayered Structures*, edited by P. Dhez and C. Weisbuch (Plenum, New York, 1988).

[3] S. P. Murarka, *Silicides for VISI Application* (Academic, Orlando, 1983).

[4] S. M. Prokes and F. Spaepen, Appl. Phys. Lett. **47**, 234 (1985).

[5] J. O. Olowafe and C. J. Mogaab, J. Appl. Phys. **72**, 4099 (1992).

[6] C. A. Ross, D. T. Wu, L. M. Goldman, and F. Spaepen, J. Appl. Phys. **72**, 2773 (1992).

[7] A. L. Greer and F. Spaepen, in *Synthetic Modulated Structure*, edited by L. L. Chang and B. C. Giessen (Academic, New York, 1985).

[8] R. G. Elliman, J. M. Gibson, D. C. Jacobson, J. M. Poate, and J. S. Williams, Appl. Phys. Lett. **46**, 4789 (1985).

[9] H. E. Cook and J. E. Hilliard, J. Appl. Phys. **40**, 2191 (1969).

[10] M. P. Rosenblum and D. Turnbull, Appl. Phys. Lett. **37**, 184 (1980).

[11] T. Novet, J. M. McConnell, and D. C. Johnson, Chem. Mater. **4**, 473 (1992).

[12] S. M. Prokes and K. L. Wang, Appl. Phys. Lett. **56**, 2628 (1990).

[13] P. C. McIntyrc, D. T. Wu, and M. Nastasi, J. Appl. Phys. **81**, 637 (1997).

[14] P. Madakson, J. Appl. Phys. **70**, 1374 (1991).

[15] W. H. Wang, H. Y. Bai, and W. K. Wang, J. Appl. Phys. **74**, 2471 (1993).

[16] M. Zhang, W. H. Wang, and W. K. Wang, Thin Solid Films **287**, 293 (1996).

[17] J. M. Baribean, R. Pascual, and S. Saimoto, Appl. Phys. Lett. **57**, 1502 (1990).

[18] E. Nygren, B. Park, L. M. Goldman, and F. Spaepen, Appl. Phys. Lett. **56**, 2094 (1990).

[19] W. L. Johnson, Mater. Sci. Eng., A **97**, 19 (1988).

[20] K. Samwer, Phys. Rep. **161**, 1 (1988).

[21] W. H. Wang, H. Y. Bai, Y. Zhang, H. Chen, and W. K. Wang, J. Appl. Phys. **73**, 4313 (1993).

[22] H. Y. Bai, W. H. Wang, and W. K. Wang, J. Mater. Res. **7**, 1423 (1992).

[23] W. H. Wang, H. Y. Bai, M. Zhang, and W. K. Wang (unpublished).

[24] H. Nakajima, M. Lkebe, Y. Muto, and H. Fujimori, J. Appl. Phys. **65**, 1637 (1989).

[25] J. W. Cahn and J. E. Hilliard, J. Chem. Phys. **28**, 258 (1958).

[26] J. W. Cahn, Acta Metall. **9**, 795 (1961).

[27] L. G. Parratt, Phys. Rev. **95**, 359 (1954).

[28] L. Nevot and P. Croce, Rev. Phys. Appl. **15**, 761 (1980).

[29] M. Veldkamp, H. Zabel, and Ch. Morawe, J. Appl. Phys. **83**, 155 (1988).

[30] J. P. Locquet, D. Nearinck, L. Stockman, Y. Bruynseaeds, and I. K. Schuller, Phys. Rev. B **39**, 13 338 (1989).

[31] G. M. Luo, M. L. Yan, W. Y. Lai, and Z. H. Mai, Phys. Rev. B **56**, 3290 (1997).

[32] H. Nakajima and H. Fujimori, *The Science Reports of the Research Institutes Tohoku University* (Tohoku University, Sendai, 1990), Vol. 35, p. 1.

[33] R. C. Cammarata, C. V. Thompson, and K. N. Tu, Appl. Phys. Lett. **51**, 1106 (1987).

[34] A. Y. Kuznetsov and B. G. Svensson, Appl. Phys. Lett. **66**, 2229 (1995).

[35] Y. Limonge, G. Brebec, and Y. Adda, in *DIMETA 82-Diffusion in Metals and Alloys*, edited by F. J. Kedves and D. L. Beke (Trans Tech, Aedermannsdorf, 1983).

[36] J. K. W. Lee, I. S. Williams, and D. J. Ellis, Nature (London) **390**, 159 (1997).

[37] J. Horvath, in *Diffusion in Solid Metals and Alloys*, edited by H. Mehrer, Landoldt-Boernstein, New Series, Group III, Vol. 26 (Springer, Berlin, 1990), p. 437.

[38] E. Weber, Appl. Phys. A: Solids Surf. **30**, 1 (1983).

[39] J. Bottiger, K. Dyrbye, K. Pampus, B. Torp, and P. H. Wiene, Phys. Rev. B **37**, 9951 (1988).

[40] S. K. Sharma, M. P. Macht, and V. Naundorf, Phys. Rev. B **46**, 3147 (1992).

[41] H. Hahn, R. S. Averback, and H. M. Shyu, J. Less-Common Met. **140**, 345 (1988).

[42] W. Dorner and H. Mehrer, Phys. Rev. B **44**, 101 (1991).

[43] S. Coffa, J. M. Poate, D. C. Jacobson, W. Frank, and W. Gustin, Phys. Rev. B **45**, 8355 (1992).

[44] A. Seeger and K. P. Chik, Phys. Status Solidi **29**, 445 (1968).

[45] K. Hoshino, R. S. Averback, H. Hahn, and S. J. Rochmen, J. Mater. Res. **xx**, 55 (1988).

[46] J. Horvath, J. Ott, K. Pfahler, and W. Ulfert, Mater. Sci. Eng. **97**, 409 (1988).

[47] H. S. Chen, Rep. Prog. Phys. **43**, 353 (1980).

[48] G. T. Hood, J. Nucl. Mater. **159**, 149 (1988).

[49] J. Utzig, J. Appl. Phys. **65**, 3868 (1988).

[50] A. M. Hollander, C. G. Duterlov, B. J. Thijsse, and E. J. Mittemeijer, Phys. Rev. B **42**, 5481 (1990).

[51] H. Hillert, Acta Metall. **9**, 525 (1961).

[52] *CRC Handbook of Chemistry and Physics*, edited by R. C. Weest (Chemical Rubber, Cleveland, 1976).

[53] S. K. Sharma, S. Banerjee, K. Jain, and A. K. Jain, J. Mater. Res. **4**, 603 (1989).

[54] A. D. Le. Claire and G. Neumann, in *Diffusion in Solid Metals and Alloys* (Ref. 37), p. 85.

[55] H. Hahn and R. S. Averback, Phys. Rev. B **37**, 6533 (1988).

[56] B. Cantor and R. W. Cahn, in *Amorphous Metallic Alloys*, edited by F. E. Luborsky (Butterworths, London, 1983), p. 487.

[57] W. Linert, Chem. Soc. Rev. **18**, 477 (1989).

[58] H. Kronmueller and W. Frank, Radiat. Eff. Defects Solids **108**, 81 (1989).

[59] S. K. Sharma, M. P. Macht, and V. Naundorf, Acta Metall. Mater. **40**, 2439 (1992).

[60] Y. Limoge, Mater. Sci. Eng., A **226–228**, 228 (1997); H. R. Schober and B. B. Laird, Phys. Rev. B **44**, 6746 (1991).

[61] M. Koiwa, Acta Metall. **22**, 1725 (1974).

[62] D. E. Polk and D. S. Boundreaux, Phys. Rev. Lett. **31**, 92 (1973).

[63] P. G. Shewmon, in *Physical Metallurgy*, edited by R. W. Cahn (North-Holland, Amsterdam, 1970).

[64] X. G. Li, Y. H. Zhang, and Y. Z. He, J. Phys.: Condens. Matter **2**, 809 (1990).

[65] C. Zener, J. Appl. Phys. **22**, 372 (1951).

[66] For details, see C. Zener, *Theory of Diffusion, Imperfections in Near Perfect Crystals* (Wiley, New York, 19xx), pp. 289–314. According to the theory for the microstructure of solid, the activation entropy ΔS consists of three parts: $\Delta S=\Delta S_a+\Delta S_b+\Delta S_c$, ΔS_a originates from the change of the atomic separation during the diffusion process, entropy increases with increasing of atomic separation, i.e., $\Delta S_a>0$; ΔS_b originates from the vibration frequency difference between the atom at perfect crystal and the atoms near the defects, $\Delta S_b=k_B\Sigma\ln(\nu_{i0}/\nu_{iv})$, where ν_{i0} is the lattice vibration frequency for the *i* atom at perfect crystal,

ν_{iv} is the atomic vibration frequency in the diffusion case, if $\nu_{iv} < \nu_{i0}$ (in the case of vacancy formation), then $\Delta S_b > 0$; if $\nu_{iv} > \nu_{iv}$ (interstitial diffusion), then $\Delta S_b < 0$. When an atom is shifted to the activation barrier height, the frequency for the atom, including the atoms nearby will be increased, i.e., the entropy decrease $\Delta S_c < 0$. In the case of collective diffusion in the ML's, the sum of the three parts is negative $\Delta S < 0$.

[67] W. L. Johnson, Mater. Sci. Prog. **30**, 81 (1986).

[68] U. Goesele and K. N. Tu, J. Appl. Phys. **53**, 3252 (1982).

[69] F. M. d'Heurle, J. Mater. Res. **3**, 167 (1988).